

A partial exploration of the potential energy surfaces of SCN and HSCN: Implications for the enzyme-mediated detoxification of cyanide

Mark A. Zottola ^{a,b,*}

^a Department of Chemistry, University of Alabama-Birmingham, Birmingham, AL 35294, United States

^b U.S. Army Medical Research Institute of Chemical Defense, 3100 Ricketts Point Road, Edgewood, MD 21010, United States

ARTICLE INFO

Article history:

Received 24 April 2009

Accepted 27 June 2009

Available online 4 July 2009

Keywords:

Cyanide

Cyanide detoxification

Rhodanese

Potential energy surface

Thiocyanate

Quantum mechanics

ABSTRACT

Cyanide (CN) is considered to be a terrorist chemical weapon due to its ready availability in multi-kilogram quantities and multi-modal means of intoxication. The body uses the sulfur transferase enzyme rhodanese to detoxify cyanide via conversion of cyanide to thiocyanate. This paper explores the potential energy surfaces for the conversion of cyanide anion and hydrogen cyanide to thiocyanate anion and thiocyanic acid, respectively.

The potential energy surface for the conversion of cyanide anion to thiocyanate shows that the formation of thiocyanate (SCN) is vastly preferred to formation of its isomer SNC. However, the potential energy surface for the conversion of hydrogen cyanide to thiocyanic acid reveals that the formation of HSCN and HNCS would be relatively equal. The failure for analytical methods to detect HNCS is rationalized by the observation that deprotonation of either HNCS or HSCN leads to the same thiocyanate anion.

© 2009 Elsevier Inc. All rights reserved.

1. Introduction

Cyanide (CN) is considered to be a military or terrorist chemical weapon [1]. Its ready availability in multi-kilogram quantities, multi-modal means of intoxication (ingested as a solution in water or inhaled as an aerosol of hydrogen cyanide gas) makes it a deadly weapon in the terrorist's arsenal.

In the body, the detoxification mechanism for cyanide is believed to involve the enzyme rhodanese [2], although mercaptopyruvate transferase [3], albumin [4] and thioredoxin [5] can also act as sulfur transfer agents. Rhodanese, an enzyme found predominantly in the mitochondria [6], mediates the conversion of CN to the substantially less toxic thiocyanate (SCN). Excretion removes the detoxification product from the body. A schematic for the mechanism of rhodanese-mediated detoxification of cyanide [7] is shown in Fig. 1.

As represented in Fig. 1, several mechanistic questions arise; does cyanide anion or hydrocyanic acid (HCN) bind to the enzyme; how does sulfur add to the bound cyanide; is the formation of an alkyl thiocyanate synchronous (one-step), or does it require several steps? The key to answering these questions is investigation of the SCN and HSCN potential energy surfaces.

Examination of the potential energy surface of thiocyanate should begin to address a number of the questions raised above. This will determine the relative stability of SNC as compared to SCN. Mapping the potential energy surface should also indicate whether SNC and SCN interconvert, and if so, how. This study will provide insights into why only SCN is observed. In addition, the question of whether cyanide or HCN binds to the enzyme can be addressed. Further, this study should determine whether the chalcogenation of cyanide is a one- or multi-step process.

2. Methods

Quantum mechanics calculations were carried out using the Gaussian G03 revision C02 [8] package. All optimizations were carried out with Cartesian polarization functions. The identity of each minimum and transition states structure was confirmed by a frequency calculation. Natural Bond Order [9] calculations were carried out using the Gaussian package. The Gaussian-produced wavefunction files were generated with Cartesian d functions and analyzed with the AIM2000 [10] software package.

3. Results and discussion

The potential energy surface for SCN was originally calculated at two different levels of theory: MPW1PW91/6-311++g(2d,p) [11] and QCISD/6-311++g(2d,p) [12]. The combination of the MPW1PW91 DFT functional and Pople basis set has been shown

* U.S. Army Medical Research Institute of Chemical Defense, 3100 Ricketts Point Road, Edgewood, MD 21010, United States. Tel.: +1 410 436 2055; fax: +1 443 617 3968.

E-mail address: Mark.Zottola@us.army.mil.

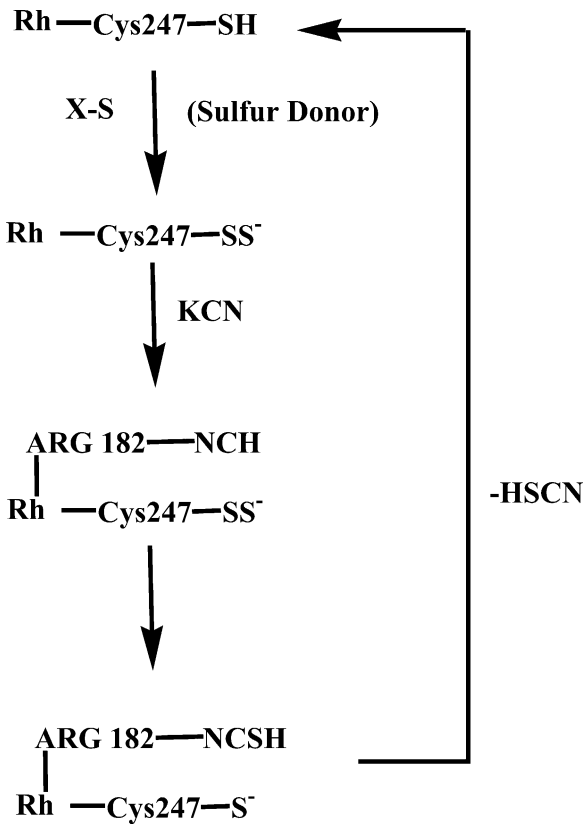


Fig. 1. This is a schematic representation of the chalcogenative detoxification of cyanide vis-à-vis rhodanese. Cysteine residue 247 reacts with a sulfur donor ($X-S$) to form the persulfide cysteine, activating the enzyme. Cyanide then binds to the enzyme. It is assumed that ARG-183 will hydrogen bond strongly to HCN, allowing a perpendicular orientation relative to the CYS-247 residue. The sulfur is then transferred to cyanide, forming thiocyanate. Thiocyanate is released from the enzyme, completing the catalytic cycle.

to be exceptional at reproducing the experimental structures of first-row hydrides [13]; the results are often superlative to higher levels of theory. The inclusion of a variational configuration interaction method (QCISD) was done to more accurately determine the structure and energy for transition state structures. While there are DFT methods parameterized for kinetic data [14], the improved energetics comes at the expense of less accurate ground state structures. The variational MPW1PW91 method allows for a reasonable computation of transition barrier heights, the results of which can be refined at the QCISD level of theory. The structures obtained from these methods are summarized in Table 1, while energy differences between structures on the potential energy surface are summarized in Table 2.

From the data in Table 2, it is clear that SCN is energetically favored over SNC by 36.0 kcal/mol after correcting for zero-point energies. This is in reasonable agreement with the energy difference computed with the QCISD method. This substantial energy difference can account for the lack of SNC observed *in vitro*.

The exploration of the SNC to SCN potential energy surface began with the assumption that a single transition state connected

Table 1

Comparison of computed structural features for minima and transition states on the SCN potential energy surface. All distances given in units of Angstroms while all angles are in units of degrees.

Compound	MPW1PW91	QCISD	QCISD(T)
SCN			
$r(S-C)$	1.661	1.679	1.686
$r(C-N)$	1.170	1.161	1.173
$\angle S-C-N$	180.0	180.0	180.0
SNC			
$r(S-N)$	1.669	1.696	1.702
$r(N-C)$	1.171	1.161	1.183
$\angle S-C-N$	180.0	180.0	180.0
INT			
$r(S-C)$	2.006	2.140	2.084
$r(S-N)$	1.944	1.956	1.998
$r(C-N)$	1.215	1.199	1.224
$\angle S-C-N$	69.32	64.75	76.42
TS1			
$r(S-C)$	1.866	1.922	1.978
$r(S-N)$	2.385	2.385	2.231
$r(C-N)$	1.195	1.193	1.210
$\angle S-N-C$	100.0	92.27	62.06
TS2			
$r(S-C)$	1.913	1.979	1.983
$r(S-N)$	2.225	2.253	2.238
$r(C-N)$	1.193	1.183	1.209
$\angle S-C-N$	88.35	87.08	85.40

Table 2

Zero-point corrected energy differences for intermediates on the S-C-N potential energy surface. Both methods used the 6-311++g(2d,p) basis set.

Transition	MPW1PW91	QCISD	QCISD(T)
SNC → TS1	26.6	26.5	27.6
INT → TS1	2.68	0.38	1.19
INT → TS2	2.00	1.40	1.29
SCN → TS2	65.3	63.0	63.7
SNC → SCN	-36.02	-35.5	-36.0

the two structures. Initial attempts to locate a single, unique SNC to SCN transition state were unsuccessful. Depending on the initial structure of the putative single transition state, two different structures were found: TS1 and TS2. TS1 was found by searching for a transition state with SNC as a starting point; TS2 was found when using SCN as a starting point. Therefore, another structure had to lie between these two transition states.

Several attempts were made to locate this structure. No second order saddle points could be found. However, perturbation of either the TS1 or TS2 structure followed by geometry optimization, lead to the identification of the same third minimum on the potential energy surface. This minimum (INT) lies between the structures TS1 and TS2 on the SCN potential energy surface. The energy for each structure is shown in Table 1 while the structures for each structure are summarized in Table 2. A representation of the computed potential energy surface is shown in Fig. 2.

The electron density topology quantities atomic monopole (charge), atomic dipole, atomic volume and electron density at the bond critical point for SCN and SNC are summarized in Table 3. The first observation made was that the electron density at the bond

Table 3

Atomic monopole and atomic dipole values (q and m , respectively) for the atoms in SCN and SNC. The electron density at the bond critical point (r) for the bonds in both SCN and SNC. All values were derived from wavefunctions computed at the MPW1PW91/6-311++g(2d,p) level of theory.

Molecule	$q(S)$	$q(N)$	$q(C)$	$\mu(S)$	$\mu(N)$	$\mu(C)$	$\rho(S-N)$	$\rho(S-C)$	$\rho(C-N)$
SCN	-0.262	-1.315	0.579	1.102	0.243	1.244		0.207	0.469
SNC	-0.112	-1.504	0.614	1.398	0.551	1.874	0.185		0.439

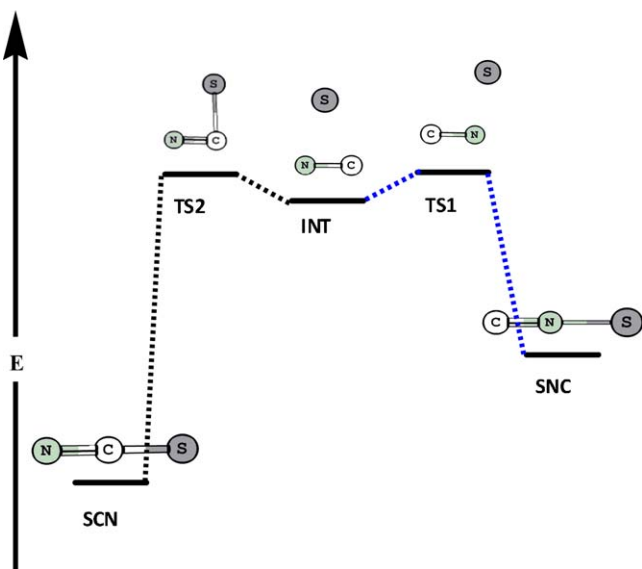


Fig. 2. This is the potential energy surface for the addition of sulfur to cyanide anion. The molecular species labeled INT is first formed. Following its formation there are two essentially rearrangement pathways having nearly identical energy barriers. The pathway to the left has sulfur migrating towards the carbon of cyanide via the transition state species labeled TS1 which leads to thiocyanate anion (labeled SNC). The pathway to the right goes through the transition state species labeled TS2 leading to the much less stable species labeled S.

critical point for the sulfur–carbon bond in SCN is 12% greater than that at the bond critical point for the sulfur–nitrogen bond in SNC. Similarly, the electron density at the bond critical point for the carbon–nitrogen in SCN is ~7% greater than that in SNC. Since the strength of a bond is proportional to the electron density at the bond critical point, the bonds in SCN are stronger than those in SNC. While this result is a consequence of SCN being more stable than SNC, it is not a cause for the difference in stability. Therefore attention was turned to probing the electron topology about each atom in SNC and SCN.

Atomic charges derived from the Bader electron-partitioning scheme [15] show that the electron distribution in SCN is significantly different than that in SNC. In SNC there is a significant accumulation of charge on nitrogen with a concomitant depletion of charge on the sulfur and carbon atoms as compared to the charges calculated for the atoms in SCN. There are two consequences of this charge redistribution. The first is that the charge on carbon in SNC is positive. This is contrary to the expectation of simple resonance theory which would predict an accumulation of charge on carbon in SNC. The depletion of more than half an electron of charge implies that the sequential arrangement of two strongly electronegative atoms adjacent to carbon overrides the resonance interaction.

The second consequence of this electron topology is an unfavorable induced dipolar interaction between sulfur and nitrogen. There are two adjacent atoms with surplus electrons. Therefore this will result in raising the kinetic energy for the electrons about sulfur and nitrogen. Raising the electronic kinetic energy will weaken the bond between these two atoms. This is corroborated by NBO analysis [9] that shows the resonance interaction in SCN is more than three times greater than that in SNC. Therefore these factors explain the weakening of bond in SNC relative to those in SCN.

Since it is assumed that a higher level of theory gives a better quality answer, the potential energy surface was recalculated using the QCISD(T) [12] level of theory. The results of these calculations are summarized in Tables 1 and 2. The apparent result from these calculations is that SCN and SNC should be produced

Table 4

Energy and structural details for structures on the HSCN potential energy surface. Bond lengths are in units of Angstroms and angles in units of degrees.

Molecule	Energy	$r(S-C)$	$r(C-N)$	$r(X-H)$	$\angle(S-C-N)$
HSCN	−491.64990	1.6939	1.1524	1.3448	176.4
HNCS	−491.67113	1.5675	1.1973	1.0047	174.3
X(TS)	−491.56630	1.6583	1.1954	1.1796 (C-H)	172.8
NPROT	−491.54756	1.9676	1.2474	1.0092	62.9
C PROT1	−491.59034	1.7482	1.2296	1.0822	80.2
C PROT3	−491.57229	1.7328	1.2625	1.0937	117.9

equally, contrary to what is experimentally observed. Clearly, chalcogenation of CN is not an appropriate model for rhodanese. Therefore, it can be reasonably assumed that HCN and not CN bind to rhodanese. This justifies examination of the HSCN potential energy surface.

Two structures were examined: INT protonated on carbon (designated as C PROT) and INT protonated on nitrogen (designated as N PROT). C PROT is the structure that should result from the addition of a sulfur atom to rhodanese-bound HCN. N PROT is the structure which would arise from isomerization of the bound HCN to bound isocyanic acid (HNC) followed by sulfur transfer from the enzyme. C PROT, N PROT as well as other minima and maxima on the HSCN potential energy surface were optimized at the MPW1PW91/6-311++g(2d,p) and QCISD/6-311++g(2d,p) levels of theory. These results are summarized in Table 4.

While it is possible that HCN isomerizes to HNC when bound, the simplest hypothesis is that the reaction results simply from enzyme-bound hydrogen cyanide. To that end, transformations from C PROT were examined in detail. Since C PROT is a nitrene, an electron deficient but neutral nitrogen species, the question arises as to whether the singlet or triplet state of this molecule was more stable. Structures for the singlet and triplet state of the nitrene were optimized using spin-unrestricted density functional theory. Since the singlet nitrene was substantially more stable than the triplet, it was assumed all reactions take place within the singlet manifold.

The potential energy surface for HSCN relevant to cyanide detoxification is shown in Fig. 3; the barrier heights for this potential energy surface within the singlet manifold are shown in Table 5. The singlet C PROT structure goes to the transition state X. Surprisingly the S–C–N angle flattens out to 180° and continues to a concave bond angle of 172.8°. A relaxed potential energy scan demonstrates that there is no saddle point before or at a 180° value for the S–C–N bond angle. X is an unusual maximum as it is a first order saddle point (i.e., a true transition state) that connects between three different minima: the starting C PROT structure, HSCN, and HNCS. Schlegel and coworkers have noted just such a phenomenon in their work on radical reactions of formaldehyde [16].

This examination sheds light on whether CN binds as the anion or as in the neutral protonated species. Were cyanide to bind as the anion, one would expect to see significant production of SNC. To date there are no reports of anything but SCN detected from the enzyme-mediated detoxification of CN.

The results presented herein predict the production of two species, HSCN and HNCS. Yet, a physiological study to detect cyanide in plasma has shown only the presence of thiocyanate

Table 5

Zero-point corrected energy differences for singlet nitrene structure conversion to HSCN and HNCS. Energy change is in units of kcal/mol.

Transition	ΔE (MPW91)	ΔE (QCISD)
C PROT1 → X	15.09	13.7
X → HSCN	−52.46	−54.03
X → HNCS	−65.78	−66.89

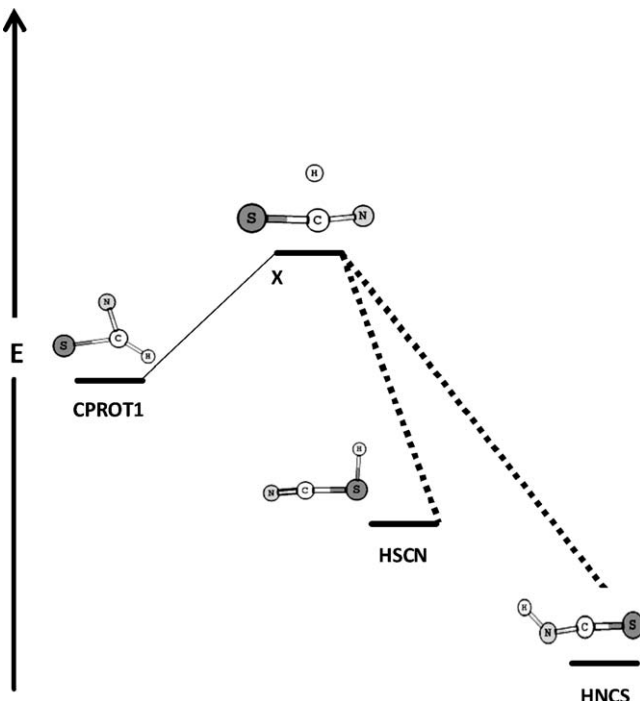


Fig. 3. This is the potential energy surface for the addition of sulfur to hydrogen cyanide. The molecular species labeled CPROT1, a nitrene, is formed first. This species then goes through the transition state labeled X. At this point, the reaction pathway can follow one of two modes. The first mode is N-H insertion leading to the product labeled HNCS. The second mode from the transition state X is C–N insertion leading to the formation of the product labeled HSCN.

anion [17]. Recent work by Logue and coworkers has examined thiocyanate content in the saliva of smokers using surface-enhanced Raman spectroscopy [18]. The Raman spectrum was most consistent with the presence of only HSCN. If these calculations were accurate, then HNCS should have been detected.

A possible explanation of this is that HNCS and HSCN could ionize to the same anion. This would be a valid explanation were HNCS more acidic than HSCN. A study by Gruber and Buss [19] showed that there was a reasonable correlation between pK_a and HOMO energy of the unionized acid for a series of carboxylic acids and phenols. Examination of the HOMO energies for both HSCN and HNCS reveals that the HOMO of HNCS is lower than the HOMO of HSCN; based on their work HNCS is expected to be more acidic than HSCN. It may well be that HNCS is formed preferentially over HSCN, albeit rapidly ionizing to form thiocyanate anion. This ionization would result in detection of only the thiocyanate anion, masking any p of HNCS.

This work has provided insight into the transformation of cyanide into thiocyanate vis-à-vis enzyme-mediated chalcogenation of HCN. These calculations have made useful predictions concerning the mechanism of transformation occurring in rhodanese. Finally this report has proposed a singlet nitrene as an intermediate for the transformation of HCN into HSCN. This is, to our knowledge, the first reported case of a nitrene being involved in a significant biological process.

Acknowledgements

The authors would like to thank Dr. Roger Klein for helpful discussions. MAZ would also like to acknowledge the Alabama Supercomputer Center for computational resources. We gratefully acknowledge funding from the National Institutes of Health and the Department of Defense (NIAID/USAMRICD Interagency agree-

ment Y1-A1-6176-01 and A120-B.P2006-01). The opinions or assertions contained herein are the private views of the authors and are not to be construed as official or as reflecting the views of the National Institutes of Health, Department of the Army, or the Department of Defense.

References

- [1] (a) M.E. Keim, Terrorism involving cyanide: the prospect of improving preparedness in the prehospital setting, *Prehosp. Disast. Med.* 21 (2006) 56–60;
 (b) R.A. Greenfield, B.R. Brown, J.B. Hutchins, J.J. Iandolo, R. Jackson, L.N. Slater, M.S. Bronze, Microbiological, biological, and chemical weapons of warfare and terrorism, *Am. J. Med. Sci.* 323 (2002) 326–340;
 (c) The Threat at Home, Often Overlooked, *Christian Science Monitor*, 29 December 2003.
- [2] (a) K. Lang, Die Rhodanide-bildung in Tiekörper, *Biochem. Ztschr.* 259 (1933) 242;
 (b) K. Lang, Die Rhodanide-bildung in Tiekörper, *Biochem. Ztschr.* 263 (1933) 262.
- [3] R. Jarabak, J. Westley, 3-Mercaptopyruvate sulfur transferase: rapid equilibrium-ordered mechanism with cyanide as the acceptor substrate, *Biochemistry* 19 (1980) 900–904.
- [4] B. Sorbo, The catalytic effect of blood serum on the reaction between colloidal sulfur and cyanide, *Acta Chem. Scand.* 9 (1955) 1656.
- [5] W.H. Watson, X. Yang, Y.E. Choi, D.P. Jones, J.P. Kehrer, Thioredoxin and its role in toxicology, *Tox. Sci.* 78 (2004) 185–188.
- [6] (a) B.H. Sorbo, Crystalline rhodanese. I. Purification and physicochemical examination, *Acta Chem. Scand.* 7 (1953) 1129;
 (b) B.H. Sorbo, Crystalline rhodanese. II. The enzyme catalyzed reaction, *Acta Chem. Scand.* 7 (1953) 1137;
 (c) A. Koj, J. Frendo, L. Wojtczak, Subcellular distribution and intramitochondrial localization of three sulfur transferases in rat liver, *FEBS Lett.* 57 (1975) 42–46.
- [7] J. Westley, *Bioorganic Chemistry*, vol. 1, Academic Press, New York, 1977.
- [8] M.J. Frisch, G.W. Trucks, H.B. Schlegel, G.E. Scuseria, M.A. Robb, J.R. Cheeseman, J.A. Montgomery Jr., T. Vreven, K.N. Kudin, J.C. Burant, J.M. Millam, S.S. Iyengar, J. Tomasi, V. Barone, B. Mennucci, M. Cossi, G. Scalmani, N. Rega, G.A. Petersson, H. Nakatsuji, M. Hada, M. Ehara, K. Toyota, R. Fukuda, J. Hasegawa, M. Ishida, T. Nakajima, Y. Honda, O. Kitao, H. Nakai, M. Klene, X. Li, J.E. Knox, H.P. Hratchian, J.B. Cross, C. Adamo, J. Jaramillo, R. Gomperts, R.E. Stratmann, O. Yazyev, A.J. Austin, R. Cammi, C. Pomelli, J.W. Ochterski, P.Y. Ayala, K. Morokuma, G.A. Voth, P. Salvador, J.J. Dannenberg, V.G. Zakrzewski, S. Dapprich, A.D. Daniels, M.C. Strain, O. Farkas, D.K. Malick, A.D. Rabuck, K. Raghavachari, J.B. Foresman, J.V. Ortiz, Q. Cui, A.G. Baboul, S. Clifford, J. Cioslowski, B.B. Stefanov, G. Liu, A. Liashenko, P. Piskorz, I. Komaromi, R.L. Martin, D.J. Fox, T. Keith, M.A. Al-Laham, C.Y. Peng, A. Nanayakkara, M. Challacombe, P.M.W. Gill, B. Johnson, W. Chen, M.W. Wong, C. Gonzalez, J.A. Pople, *Gaussian 03, Revision C.02*, Gaussian, Inc., Wallingford, CT, 2004.
- [9] (a) A.E. Reed, L.A. Curtiss, F. Weinhold, *Chem. Rev.* 88 (1988) 899;
 (b) F. Weinhold, C.R. Landis, Valence and bonding, in: *A Natural Bond Orbital Donor-Acceptor Perspective*, University Press, Cambridge, UK, 2005.
- [10] F. Biegler-Koenig, J. Schoenbohm, AIM2000 Version 2.0, Copyright® (2002).
- [11] V.A. Rassolov, J.A. Pople, J. Ratner, *J. Chem. Phys.* 109 (1998) 1223.
- [12] J.A. Pople, M. Head-Gordon, K. Raghavachari, *J. Chem. Phys.* 87 (1987) 5968.
- [13] R.A. Klein, M.A. Zottola, Pople versus Dunning basis-sets for group IA metal hydrides and some other second row hydrides: the case against a De Facto standard, *Chem. Phys. Lett.* 419 (2005) 254.
- [14] (a) B.J. Lynch, P.L. Fast, M. Harris, D.G. Truhlar, Adiabatic connection for kinetics, *J. Chem. Phys.* A 115 (2000) 4811;
 (b) Y. Zhao, B.J. Lynch, D.G. Truhlar, Development and assessment of a new hybrid density functional model for thermochemical kinetics, *J. Chem. Phys.* A 108 (2004) 2715;
 (c) Y. Zhao, J. Pu, J.B. Lynch, D.G. Truhlar, Tests of second-generation and third-generation density functionals for thermochemical kinetics, *Phys. Chem. Chem. Phys.* 6 (2004) 673;
 (d) Y. Zhao, D.G. Truhlar, Hybrid meta density functional theory methods for thermochemistry, thermochemical kinetics and noncovalent interactions: the MPW1B95 and MPWB1K models and comparative assessments for hydrogen bonding and van der Waals interactions, *J. Chem. Phys.* A 108 (2004) 6908.
- [15] (a) R.F.W. Bader, W.H. Henneker, P.E. Cade, Molecular charge distributions and chemical binding, *J. Chem. Phys.* 46 (1967) 3341;
 (b) R.F.W. Bader, H.J.T. Preston, Determination of the charge distribution of methane by a method of density constraints, *Theor. Chim. Acta* 17 (1970) 384.
- [16] J. Li, X. Li, S. Shaik, H.B. Schlegel, Single transition state serves two mechanisms. Ab initio classical trajectory calculations of the substitution-electron transfer branching ratio in $\text{CH}_2\text{O}^+ + \text{CH}_3\text{Cl}$, *J. Phys. Chem. A* 108 (2004) 8526.
- [17] W.A. Groff Sr., F.W. Stemler, A. Kaminski, H.L. Froehlich, R.P. Johnson, Plasma free cyanide and blood total cyanide: a rapid completely automated microdistillation assay, *Toxicol. Clin. Toxicol.* 23 (1985) 133.
- [18] B. Logue, private communication.
- [19] C. Gruber, V. Buss, Quantum-mechanically calculated properties for the development of quantitative structure-activity relationships (QSARs). pK_a -values of phenols and aromatic and aliphatic carboxylic acids, *Chemosphere* 19 (1989) 1595.